

A Noise-Aware Scalable Subspace Classical Optimizer for the Quantum Approximate Optimization Algorithm*

K. J. Dzahini [†]J. M. Larson [†]M. Menickelly [†]S. M. Wild [‡]

August 19, 2025

Abstract: We introduce ANASTAARS, a noise-aware scalable classical optimizer for variational quantum algorithms such as the quantum approximate optimization algorithm (QAOA). ANASTAARS leverages adaptive random subspace strategies to efficiently optimize the ansatz parameters of a QAOA circuit, in an effort to address challenges posed by a potentially large number of QAOA layers. ANASTAARS iteratively constructs random interpolation models within low-dimensional affine subspaces defined via Johnson–Lindenstrauss transforms. This adaptive strategy allows the selective reuse of previously acquired measurements, significantly reducing computational costs associated with shot acquisition. Furthermore, to robustly handle noisy measurements, ANASTAARS incorporates noise-aware optimization techniques by estimating noise magnitude and adjusts trust-region steps accordingly. Numerical experiments demonstrate the practical scalability of the proposed method for near-term quantum computing applications.

Keywords Quantum Approximate Optimization Algorithm · Classical Optimizers for QAOA · Randomized Subspace Algorithms

*This material was based upon work supported by the U.S. Department of Energy, Office of Science, Office of Advanced Scientific Computing Research Applied Mathematics and ARQC programs under Contract Nos. DE-AC02-06CH11357 and DE-AC02-05CH11231.

[†]Argonne National Laboratory, 9700 S. Cass Avenue, Lemont, IL 60439, USA.

[‡]Lawrence Berkeley National Laboratory, 1 Cyclotron Road, Berkeley, CA 94720, USA.

1 Introduction

Remarkable progress has been made in the design of noisy intermediate-scale quantum (NISQ) devices while large-scale, fault-tolerant quantum computers are still far from being available. Interest in developing practical algorithms designed for NISQ devices is on the rise. Variational quantum algorithms (VQAs) [6, 8, 14, 34] were introduced to exploit the capabilities of current quantum systems using a hybrid quantum-classical optimization process. In a VQA, the hybrid cycle involves executing a parameterized circuit on a quantum computer and using an optimizer on a classical machine to update the circuit parameters by minimizing a cost function based on the quantum circuit outputs. This approach allows VQAs to benefit from the use of shallow quantum circuits, making them less vulnerable to noise in NISQ devices [7]. VQAs exhibit promise for quantum simulations aimed at finding the ground state energies of complex molecules, as well as for solving difficult binary optimization problems such as MaxCut variants [52, 54].

As one of the most promising VQAs, the quantum approximate optimization algorithm (QAOA) [22] has attracted significant interest and has numerous and far-reaching applications. As emphasized in [7], in addition to MaxCut problems, QAOA is well suited for finding good approximate solutions to various optimization problems, most broadly encapsulated by quadratic unconstrained binary optimization problems (see [7] and references therein). QAOA is intended to find approximate solutions to difficult combinatorial optimization problems on quantum computers by encoding the problem’s Hamiltonian into a quantum circuit and utilizing adiabatic time evolution to optimize the circuit’s variational parameters. An approximate solution is then obtained by measuring the QAOA circuit using the parameters identified by a classical numerical optimization algorithm, which aims to optimize a problem-specific and well-designed cost function. However, the optimization methods employed must be both robust and efficient in navigating a cost function landscape that is typically periodic and nonconvex, since these are typical characteristics of the loss landscape [31, 51]. Moreover, quantum measurements are inherently stochastic, meaning the cost function values used by QAOA are typically statistical estimates derived from repeated measurements (shots) of the quantum circuit’s output state, which inevitably introduce stochastic noise into the optimization process.

In this manuscript our focus is on the classical numerical optimization method, which plays a crucial role in the QAOA framework. Choosing the right optimization method is critical for improving QAOA performance. Current strategies for enhancing QAOA parameters can be broadly classified into three categories [7]: machine learning (ML), gradient-based, and derivative-free approaches, with the last referring to optimization methods that do not require any derivative information from the user or the cost function oracle. Although ML methods can speed up QAOA optimization by leveraging correlations and patterns among parameters, they may encounter scalability challenges, particularly for more complex problems, and often require numerous training instances to achieve good performance. On the other hand, commonly used gradient-based methods such as stochastic gradient descent or BFGS can be more robust to noise and problem variations [39, 41]. However, gradient-based methods can be computationally expensive and sensitive to noise in NISQ devices and often require a large number of measurements to compute via the parameter shift rule [55]. Some researchers have attempted to adaptively select shot counts in the computation of such noisy gradients [1, 29]. As an alternative, given the difficulty in obtaining accurate gradients, practitioners often rely on derivative-free optimization (DFO) methods [3, 16, 30] as the classical optimizer in VQAs [31]. Examples of such methods include the popular model-based trust-region (MBTR) algorithm BOBYQA [45], as well as COBYLA [25, 42, 43], NEWUOA [44], SB-PLX [48], PRAXIS [9], and Nelder–Mead [40], which were recently benchmarked as QAOA optimizers by Shaydulin et al. [51]. Their study revealed that QAOA’s performance deteriorates significantly as the number of layers increases, indicating the difficulty of parameter optimization even at relatively shallow circuit depths. The software package `scikit-quant` [32], on the other hand, integrates various DFO optimizers, which the authors have found to be effective for optimizing variational parameters within the VQA framework. We note that although none of the aforementioned DFO methods are specifically designed for stochastic optimization, they are often found to be far more efficient than their stochastic counterparts. However, any method designed for a deterministic problem will not resample a cost function at the same parameter setting more than once. Consequently, deterministic methods are inevitably prone to becoming “stuck” in the presence of stochastic noise. These observations motivated the development of ANATRA [31], an algorithm for noisy DFO problems that encompass those presented by VQAs. ANATRA was shown to outperform many state-of-the-art deterministic and stochastic optimizers on QAOA problems, particularly in high-noise environments.

The performance of QAOA is typically assessed through the ratio of the expectation value of the globally optimal QAOA solution to the globally optimal value of the original optimization problem. This ratio asymptotically improves as the number of layers, p , increases, as QAOA recovers the aforementioned adiabatic evolution when p approaches infinity [7]. The latter observation suggests that creating greater depth circuits by increasing p , which entails solving correspondingly higher-dimensional optimization problems, would guarantee better ratios. However, performance guar-

antees of DFO methods, including all of those mentioned above, scale polynomially in dimension p . The situation is exacerbated by stochastic noise in a QAOA framework, since performance guarantees for stochastic DFO are considerably weakened. These observations shape our primary goal in this work, which is to develop a stochastic DFO algorithm capable of solving *high-dimensional* stochastic problems.

In this work we introduce **ANASTAARS**, a Noise-Aware Stochastic Trust-region Algorithm using Adaptive Random Subspaces. **ANASTAARS** is based on the existing **STARS** [18] algorithmic framework, achieving scalability by optimizing random models that approximate the cost function within low-dimensional affine subspaces. Limiting model construction to subspaces significantly reduces per-iteration costs in terms of function evaluations. In contrast to the **STARS** algorithmic framework and previous work involving random subspaces with fixed dimensions (see [12, 13, 47, 49] and the **RSDFO(-GN)** framework [10]), **ANASTAARS** employs an *adaptive* subspace dimension selection strategy similar to that used in **DF-BGN** [10], as well as subspace variants of **POUNDERs** [36, 37]. Instead of generating a completely new poised set of interpolation points at each iteration, the proposed method updates the model by generating only a few or even a single new interpolation point, reusing past points (and their corresponding function values) from strictly lower-dimensional subspaces in such a way that the resulting set remains poised. This approach not only introduces a novel way to reduce per-iteration costs in terms of function evaluations but also avoids constructing random models in fixed-dimension subspaces, resulting in an efficient optimization process through the use of adaptive subspace models. Furthermore, to address the observation that model-based methods perform well when the signal-to-noise ratio is high, as emphasized in [31], **ANASTAARS** incorporates a strategy from the noise-aware numerical optimization literature by utilizing an estimate of the noise level in function evaluations.

2 Background

2.1 The Quantum Approximate Optimization Algorithm

Introduced by Farhi et al. [22], QAOA is a VQA aimed at solving combinatorial optimization problems by preparing a parameterized quantum circuit, designed so that high-quality solutions to the optimization problem correspond to modes of measurements. Alongside an initial state $|\psi_0\rangle$ and a hyperparameter p representing the number of layers, the circuit is determined by operators \mathbf{H}_P and \mathbf{H}_M , respectively the problem Hamiltonian and the mixer Hamiltonian. The prepared quantum state is

$$|\psi(\gamma, \beta)\rangle = e^{-i\beta_p \mathbf{H}_M} e^{-i\gamma_p \mathbf{H}_P} \dots e^{-i\beta_1 \mathbf{H}_M} e^{-i\gamma_1 \mathbf{H}_P} |\psi_0\rangle, \quad (1)$$

with $\gamma = (\gamma_1, \dots, \gamma_p)^\top$ and $\beta = (\beta_1, \dots, \beta_p)^\top$ denoting free parameters. In the QAOA circuit with properly tuned parameters, $|\psi(\gamma, \beta)\rangle$ converges to the ground state of the problem Hamiltonian \mathbf{H}_P as the number of layers p increases toward infinity. By design of the cost function, the energy of the problem Hamiltonian approaches the optimal value of the optimization problem's objective function. A classical optimization algorithm is used to tune the variational parameters β and γ by solving the problem

$$\min_{\gamma, \beta} \{ \langle \psi(\gamma, \beta) | \mathbf{H}_P | \psi(\gamma, \beta) \rangle \}, \quad (2)$$

where the cost function in (2) represents the expectation of the energy. The cost function can only be sampled in practice. During each QAOA iteration, the expected value

$$f(\gamma_1, \dots, \gamma_p, \beta_1, \dots, \beta_p) = \langle \psi(\gamma, \beta) | \mathbf{H}_P | \psi(\gamma, \beta) \rangle$$

is estimated from multiple measurements of $|\psi(\gamma, \beta)\rangle$ and provided to the classical optimizer as the cost function. In other words, if $\mathbf{x} = (\gamma_1, \dots, \gamma_p, \beta_1, \dots, \beta_p)^\top \in \mathbb{R}^d$ with $d = 2p$, the classical optimizer aims to solve the stochastic optimization problem

$$\min_{\mathbf{x} \in \mathbb{R}^d} f(\mathbf{x}) \quad \text{with} \quad f(\mathbf{x}) = \mathbb{E}_{\underline{\theta}} [f_{\underline{\theta}}(\mathbf{x})], \quad (3)$$

while having access only to the noisy function values $f_{\underline{\theta}}(\mathbf{x})$, where $\underline{\theta}$ is a random variable modeling the stochasticity from the aforementioned measurements. Note that each individual measurement corresponds to a complete execution of the circuit (a shot).

A problem frequently considered in the context of QAOA is the weighted MaxCut. We define an instance of MaxCut as follows.

MaxCut. Consider an undirected graph $G = (V, E)$ where V is the set of vertices identified with $V = [n]$ and E is the set of edges. Denote by w_{uv} the weight associated with each edge $(u, v) \in E$, which connects the vertices u and v . Find $\mathbf{s} := (s_1, \dots, s_n) \in \{-1, 1\}^n$ that maximizes

$$h(\mathbf{s}) = \sum_{(u,v) \in E} \frac{w_{uv}}{2} (1 - s_u s_v).$$

The Hamiltonian \mathbf{H}_P encoding the MaxCut problem on qubits is obtained by mapping spin variables s_i onto the spectrum of Pauli- \mathbf{Z} matrices; that is,

$$\mathbf{H}_P = \sum_{(u,v) \in E} \frac{w_{uv}}{2} (\mathbf{I} - \mathbf{Z}_u \mathbf{Z}_v),$$

where \mathbf{Z}_u is the Pauli- \mathbf{Z} operator acting on the u th qubit. The mixer Hamiltonian \mathbf{H}_M is defined as

$$\mathbf{H}_M = \sum_{i \in V} \mathbf{X}_i, \quad (4)$$

where \mathbf{X}_i is the Pauli- \mathbf{X} operator acting on the i th qubit. The initial state $|\psi_0\rangle$ is chosen as the ground state of the mixer Hamiltonian, which for \mathbf{H}_M in Equation (4) is

$$|\psi_0\rangle = |+\rangle^{\otimes n} := \frac{1}{\sqrt{2^n}} \sum_{\mathbf{x} \in \{0,1\}^n} |\mathbf{x}\rangle.$$

2.2 Subspace Model-Based Stochastic Trust-Region Methods

As discussed in Section 1, DFO methods for deterministic cost functions can be more shot-efficient than those tailored for stochastic optimization. Some of the most successful approaches are adaptations of the model-based trust-region (MBTR) framework [16], with notable implementations pioneered by Michael Powell. For noise-free settings such methods typically require a number of evaluations that is polynomial in the dimension d ; methods for noisy problems often require significantly more samples. Our primary concern in designing a novel algorithm is to be deliberately noise-aware, since MBTR methods, traditionally developed for deterministic problems, eventually get “stuck” in the presence of noise, as discussed in Section 1. Dzhahini and Wild [18] took a step in this direction with the design of STARS, where scalability is achieved by iteratively constructing and minimizing stochastic models that approximate the cost function within low-dimensional random subspaces, in contrast to earlier methods [5, 15, 50] that utilize “full-space” models.

Indeed, it has been established that in a simple stochastic noise framework [23, 38], obtaining good full-space models at each iteration k of a standard model-based method (applied to (3)) requires at least $\Omega((d+1) \max\{\delta_k^{-2}, \delta_k^{-4}\} (1 - \alpha^{1/(d+1)}))$ function evaluations, for fixed $\alpha \in (0, 1)$ and $\delta_k > 0$ a measure of locality, with d replaced by $q \ll d$ in the above quantity for STARS subspace models. This shows in particular the low per-iteration cost of building the subspace models compared with full-space ones, especially since q can be chosen independently of d .

To solve Problem (3), the STARS framework, which inspires the algorithm proposed in the present work, operates as follows. At each iteration k , given an incumbent point $\mathbf{x}_k \in \mathbb{R}^d$ and a realization $\mathbf{Q}_k \in \mathbb{R}^{d \times q}$ of a specific random matrix $\underline{\mathbf{Q}}_k$ (where the general random variable is denoted with an underbar), an interpolation model \hat{m}_k is built on the affine subspace $\mathcal{Y}_k := \{\mathbf{x}_k + \mathbf{Q}_k \mathbf{s} : \mathbf{s} \in \mathbb{R}^q\}$ using realizations of the noisy function f_Q . This model is typically quadratic and is given by

$$\hat{m}_k(\mathbf{s}) := \mathbf{f}_k + \hat{\mathbf{g}}_k^\top \mathbf{s} + \frac{1}{2} \mathbf{s}^\top \hat{\mathbf{H}}_k \mathbf{s} \approx f(\mathbf{x}_k + \mathbf{Q}_k \mathbf{s}), \quad (5)$$

with $\hat{\mathbf{g}}_k \approx \mathbf{Q}_k^\top \nabla f(\mathbf{x}_k) \in \mathbb{R}^q$ and $\hat{\mathbf{H}}_k \in \mathbb{R}^{q \times q}$ respectively denoting the low-dimensional model gradient and Hessian. These two defining quantities and the scalar \mathbf{f}_k consist of $\frac{1}{2}(q+1)(q+2)$ parameters, which are obtained by solving linear interpolation systems of this size; this size also corresponds to the number of estimates of f that are employed and thus directly informs the number of shots employed in model construction. As we emphasize below, when $q \ll d$ there are significantly fewer model parameters (and hence fewer shots employed by any one model) than there are for full-space models (i.e., when $q = d$).

The model \hat{m}_k is used to approximate the cost function f in the *trust region* $\mathcal{B}(\mathbf{x}_k, \delta_k; \mathbf{Q}_k) := \{\mathbf{x}_k + \mathbf{Q}_k \mathbf{s} \in \mathcal{Y}_k : \|\mathbf{s}\|_2 \leq \delta_k\}$, where $\delta_k > 0$ denotes the trust-region radius. A trial step is obtained from the (approximate) solution of $\mathbf{s}_k \approx \arg \min \{\hat{m}_k(\mathbf{s}) : \mathbf{s} \in \mathbb{R}^q, \|\mathbf{s}\|_2 \leq \delta_k\}$. Estimates $f_k^0 \approx f(\mathbf{x}_k)$ and $f_k^s \approx f(\mathbf{x}_k + \mathbf{Q}_k \mathbf{s}_k)$ are computed using evaluations of the noisy function f_θ . The potential change in f due to the trial step \mathbf{s}_k is assessed by comparing a preset value $\eta_1 \in (0, 1)$ with the ratio $\rho_k := \frac{f_k^0 - f_k^s}{\hat{m}_k(\mathbf{0}) - \hat{m}_k(\mathbf{s}_k)}$ of the reduction in the estimates with the reduction in the model. If the ratio is greater than η_1 , then the iteration is declared successful, in which case the incumbent is replaced by the trial step, and the trust-region radius is not decreased. Otherwise, the trust-region radius is decreased, and the incumbent remains unchanged. An instantiation of STARS is presented in Algorithm 1.

As emphasized in [18, Section 3.1], the success of an algorithm in the STARS framework requires that the subspace \mathcal{Y}_k defined by the span of the columns of \mathbf{Q}_k must be aligned with the gradient $\nabla f(\mathbf{x}_k)$ in order to ensure sufficient decrease in f . By alignment, we mean that

$$\|\mathbf{Q}_k^\top \nabla f(\mathbf{x}_k)\| \geq \epsilon \|\nabla f(\mathbf{x}_k)\|, \quad (6)$$

which means that the subspace-reduced gradient norm is close to the full-space gradient norm in a relative sense. If the converse of the event (6) were to occur sufficiently often, then an algorithm in the STARS framework could not converge. Therefore, we assume that the random matrix \mathbf{Q}_k with realizations $\mathbf{Q}_k \in \mathbb{R}^{d \times q}$ determining the subspace satisfies the following so-called well-alignment condition.

Definition 2.1. (Simplified version of [18, Definition 3.2]) For fixed $\epsilon, \beta \in (0, 1/2)$, a sequence $\{\mathbf{Q}_k\}_{k \in \mathbb{N}}$ of random matrices, with $\mathbf{Q}_k \in \mathbb{R}^{d \times q}$, is $(1 - \beta)$ -probabilistically ϵ -well aligned if, for any $\mathbf{v} \in \mathbb{R}^d$,

$$\mathbb{P} \left(\left\| \mathbf{Q}_k^\top \mathbf{v} \right\|_2 \geq \epsilon \|\mathbf{v}\|_2 \right) \geq 1 - \beta. \quad (7)$$

Matrices satisfying (7) will be referred to as $WAM(\epsilon, \beta)$.

It follows from (7) that in the particular case $\mathbf{v} = \nabla f(\mathbf{x}_k)$ and β small enough, with high probability, $\|\mathbf{Q}_k^\top \nabla f(\mathbf{x}_k)\|$ is bounded away from zero whenever $\nabla f(\mathbf{x}_k) \neq 0$, as desired. Fortunately, the existence of random matrices satisfying (7) is guaranteed, for example, by the celebrated Johnson–Lindenstrauss lemma [26], reported in [27] and recalled next.

Lemma 2.1. (Johnson–Lindenstrauss [27, Lemma 1]) For any integer $d > 0$ and $0 < \epsilon, \beta < 1/2$, there exists a probability distribution on $d \times q$ real matrices for $q = \Theta(\epsilon^{-2} \log(1/\beta))$ such that for any $\mathbf{v} \in \mathbb{R}^d$ and any matrix \mathbf{Q} drawn from the aforementioned distribution

$$\mathbb{P} \left((1 - \epsilon) \|\mathbf{v}\|_2 \leq \left\| \mathbf{Q}^\top \mathbf{v} \right\|_2 \leq (1 + \epsilon) \|\mathbf{v}\|_2 \right) \geq 1 - \beta. \quad (8)$$

[0] Initialization

Choose algorithmic parameters and a starting point $\mathbf{x}_0 \in \mathbb{R}^d$, fix a subspace dimension $q \in \llbracket 1, d \rrbracket$, and set the iteration counter $k \leftarrow 0$.

[1] Subspace model, estimates, and updates

Generate $\mathbf{Q}_k \in \mathbb{R}^{d \times q}$ using Haar measure to build the model $\hat{m}_k : \mathbb{R}^q \rightarrow \mathbb{R}$.

Minimize \hat{m}_k in a trust region to obtain \mathbf{s}_k .

Obtain accurate estimates $f_k^0 \approx f(\mathbf{x}_k)$ and $f_k^s \approx f(\mathbf{x}_k + \mathbf{Q}_k \mathbf{s}_k)$.

Use $\rho_k = \frac{f_k^0 - f_k^s}{\hat{m}_k(\mathbf{0}) - \hat{m}_k(\mathbf{s}_k)}$ and $\|\mathbf{g}_k\|_2$ to check whether the iteration is successful or not.

Set $\mathbf{x}_{k+1} = \mathbf{x}_k + \mathbf{Q}_k \mathbf{s}_k$ (**success**) and $\mathbf{x}_{k+1} = \mathbf{x}_k$ (**failure**).

Update the trust-region radius. Set $k \leftarrow k + 1$, and go to [1].

Algorithm 1: Simplified STARS algorithm [18].

Various distributions, such as Gaussian matrices [18, Theorem 3.4], matrices generated by hashing and hashing-like approaches [20, 27], and Haar distribution orthogonal matrices [35] are commonly used for generating random matrices that satisfy (7). The last strategy, used in the proposed ANASTAARS algorithm, is presented in the result stated next. We first recall the Haar measure, which is the unique translation-invariant probability measure on the compact group $\mathcal{O}(d)$ or orthogonal matrices.

Theorem 2.1. ([19, Theorem 2.2], inspired by [35, Lemma 6.1]) Let $\epsilon, \beta \in (0, 1/2)$ and $\mathbf{U} := (\mathbf{U}_{ij})_{1 \leq i, j \leq d} \in \mathbb{O}(d)$ be a Haar-distributed matrix. Let $\mathbf{U}_{q \times d} \in \mathbb{R}^{q \times d}$ be the matrix consisting of the first q rows of \mathbf{U} , and define $\mathbf{Q}^\top := \sqrt{\frac{d}{q}} \mathbf{U}_{q \times d}$. Then there exists an absolute constant $\eta > 0$ such that if $q \geq \frac{4}{\eta} \epsilon^{-2} \log(2/\beta)$, then for all $\mathbf{v} \in \mathbb{R}^d$, (8) holds.

For theoretical purposes and practical efficiency, the estimates f_k^0 and f_k^s are required to be sufficiently close to their corresponding estimated function values by satisfying so-called ϵ_f -accuracy conditions [18, Definition 3.12], [4, 15, 17, 21]. More precisely, given $\epsilon_f > 0$ and $\delta_k > 0$, the estimates $f_k^0 \approx f(\mathbf{x}_k)$ and $f_k^s \approx f(\mathbf{x}_k + \mathbf{Q}_k \mathbf{s}_k)$ must satisfy

$$|f_k^0 - f(\mathbf{x}_k)| \leq \epsilon_f \delta_k^2 \quad \text{and} \quad |f_k^s - f(\mathbf{x}_k + \mathbf{Q}_k \mathbf{s}_k)| \leq \epsilon_f \delta_k^2,$$

in which case they are called ϵ_f -accurate. Given that $f(\mathbf{x}_k)$ and $f(\mathbf{x}_k + \mathbf{Q}_k \mathbf{s}_k)$ are not accessible in practice, the above conditions are satisfied only in probability. Such estimates are obtained by averaging samples or realizations of the noisy function. For example, for an appropriate sample size π_k , $f_k^0 = \frac{1}{\pi_k} \sum_{\ell=1}^{\pi_k} f_{\theta_\ell^0}(\mathbf{x}_k)$, where the θ_ℓ^0 are realizations of independent random samples of θ . For details on how random estimates f_k^0 and f_k^s with respective realizations f_k^0 and f_k^s can be generated, see [4, Section 2.3], [15, Section 5], and [21, Section 5.1]. On the other hand, the model \hat{m}_k is required to be fully linear (see, e.g., [18, Definition 3.10]), a condition that amounts to the model satisfying similar error bounds as a first-order Taylor model. Full linearity is achieved, for instance, and as employed in this paper (see Section III), by using a linear model interpolating function values on a set of points of appropriate geometry.

3 Subspace Model Construction Leading to Adaptive Subspace Selection

A key contribution of this paper is the development of strategies that enable the reuse of interpolation points (and their corresponding function values, thus reducing the number of shots required by the algorithm) from an unsuccessful iteration k to construct higher-dimensional subspace models in the subsequent iteration $k+1$. Unlike prior works that use a fixed subspace dimension, the proposed strategies result in a low per-iteration cost in ANASTAARS in terms of function evaluations/shots. Below, for all $i = 0, 1, \dots$, the $\theta_{k,\ell}^i$, $\ell = 1, 2, \dots$, are realizations of independent random samples of $\theta_{k,\ell}^i$ of the independent random variables θ_k^i distributed as θ . Unless otherwise stated, $\mathbf{Q}_k = \sqrt{\frac{d}{q}} \mathbf{U}_k \in \mathbb{R}^{d \times q}$ with $q < d$, where \mathbf{U}_k is a realization of a random matrix \mathbf{U}_k obtained from Haar distribution (see Theorem 2.1), and hence the columns of \mathbf{U}_k are orthonormal. We define $\mathbf{1}_q := (1, \dots, 1)^\top \in \mathbb{R}^q$, $\mathbf{0}_q = (0, \dots, 0)^\top \in \mathbb{R}^q$ and $\hat{q} := \sqrt{1 + \frac{1}{q}}$. $\mathbf{I}_q \in \mathbb{R}^{q \times q}$ as the identity matrix. \mathcal{P}_q^2 is the space of polynomials of degree less than or equal to 2 in \mathbb{R}^q .

3.1 Subspace Linear Models

The linear model construction (at iteration k) described next is inspired by [18, Theorem 3.16]. At each point of a poised set¹ $\mathbb{S}_k^q := \{\mathbf{s}_k^0, \mathbf{s}_k^1, \dots, \mathbf{s}_k^q\} \subseteq \mathbb{R}^q \cap \mathcal{B}(\mathbf{0}, \delta_k)$, with $\mathbf{s}_k^0 = \mathbf{0}$, let $f_k^s(\mathbf{s}_k^i; \theta_k^i) := \frac{1}{\pi_k} \sum_{\ell=1}^{\pi_k} f_{\theta_{k,\ell}^i}(\mathbf{x}_k + \mathbf{Q}_k \mathbf{s}_k^i)$. A linear model

$$\hat{m}_k(\mathbf{s}) = \mathbf{a}_k^0 + \mathbf{a}_k^\top \mathbf{s}, \quad (\mathbf{a}_k^0, \mathbf{a}_k) \in \mathbb{R} \times \mathbb{R}^q,$$

is built by fitting values of $\mathbf{a}_k^0, \mathbf{a}_k$, such that $\hat{m}_k(\mathbf{s}_k^i) = f_k^s(\mathbf{s}_k^i; \theta_k^i)$ for all $\mathbf{s}_k^i \in \mathbb{S}_k^q$. That is, $\mathbf{a}_k^0 = f_k^s(\mathbf{s}_k^0; \theta_k^0)$ while $\mathbf{a}_k = \nabla \hat{m}_k(\mathbf{s})$ is obtained by solving the $q \times q$ linear system

$$\mathbf{L}_k^\top \mathbf{a}_k = \delta f_k(\mathbb{S}_k^q; \theta_k) := \begin{bmatrix} f_k^s(\mathbf{s}_k^1; \theta_k^1) - f_k^s(\mathbf{s}_k^0; \theta_k^0) \\ f_k^s(\mathbf{s}_k^2; \theta_k^2) - f_k^s(\mathbf{s}_k^0; \theta_k^0) \\ \vdots \\ f_k^s(\mathbf{s}_k^q; \theta_k^q) - f_k^s(\mathbf{s}_k^0; \theta_k^0) \end{bmatrix} \in \mathbb{R}^q,$$

where $\mathbf{L}_k := [\mathbf{s}_k^1 - \mathbf{s}_k^0 \dots \mathbf{s}_k^q - \mathbf{s}_k^0] \in \mathbb{R}^{q \times q}$.

Recall from Algorithm 1 that on any unsuccessful iteration k , we have $\mathbf{x}_{k+1} = \mathbf{x}_k$. Inspired by the *explicit geometric construction* of Haar measure [35, Section 1.2], we set

$$\mathbf{Q}_{k+1} := \sqrt{\frac{d}{q+1}} [\mathbf{U}_k, \boldsymbol{\mu}_{k+1}] \in \mathbb{R}^{d \times (q+1)} \quad (9)$$

¹Poisedness can be understood as a nonzero volume of the convex hull of the interpolation points; see, e.g., [30, Section 2.2] for more details.

after an unsuccessful iteration, where $\boldsymbol{\mu}_{k+1}$ is a realization of a random vector uniformly distributed on the intersection of the d -dimensional sphere and the orthogonal complement \mathbf{U}_k^\perp .

Analogous to the construction of \hat{m}_k , using

$$\mathbb{S}_{k+1}^{q+1} := \left\{ \mathbf{s}_{k+1}^i = \begin{bmatrix} \hat{q} \mathbf{s}_k^i \\ 0 \end{bmatrix}, \mathbf{s}_{k+1}^{q+1} = \begin{bmatrix} \mathbf{0}_q \\ \zeta_{k+1} \end{bmatrix} : \mathbf{s}_k^i \in \mathbb{S}_k^q, 0 < |\zeta_{k+1}| \leq \delta_k \right\},$$

we construct a $(q+1)$ -dimensional subspace linear model \hat{m}_{k+1} defined by

$$\hat{m}_{k+1}(\mathbf{s}) = \mathbf{a}_{k+1}^0 + \mathbf{a}_{k+1}^\top \mathbf{s}, \quad (\mathbf{a}_{k+1}^0, \mathbf{a}_{k+1}) \in \mathbb{R} \times \mathbb{R}^{q+1}.$$

Note that

$$\mathbf{x}_{k+1} + \mathbf{Q}_{k+1} \mathbf{s}_{k+1}^i = \mathbf{x}_k + \mathbf{Q}_k \mathbf{s}_k^i, \quad i = 0, 1, \dots, q, \quad (10)$$

and so the construction of \hat{m}_{k+1} reuses past points $\mathbf{x}_k + \mathbf{Q}_k \mathbf{s}_k^i$ and their corresponding function values $f_k^s(\mathbf{s}_k^i; \theta_k^i)$, in addition to one new point $\mathbf{x}_{k+1} + \mathbf{Q}_{k+1} \mathbf{s}_{k+1}^{q+1} = \mathbf{x}_k + \sqrt{\frac{d}{q+1}} \boldsymbol{\mu}_{k+1} \zeta_{k+1}$ and its corresponding function value $f_k^s(\mathbf{s}_{k+1}^{q+1}; \theta_{k+1}^{q+1})$. Thus, the resulting linear interpolation system for constructing \hat{m}_{k+1} defined by \mathbf{a}_{k+1}^0 and $\mathbf{a}_{k+1}^\top := [(\mathbf{a}_{k+1}^q)^\top \mathbf{a}_{k+1}^1]^\top$ is only a $(q+1) \times (q+1)$ linear system:

$$\begin{bmatrix} \hat{q} \mathbf{L}_k^\top & \mathbf{0}_q \\ \mathbf{0}_q^\top & \zeta_{k+1} \end{bmatrix} \begin{bmatrix} \mathbf{a}_{k+1}^q \\ \mathbf{a}_{k+1}^1 \end{bmatrix} = \begin{bmatrix} \boldsymbol{\delta}^{f_k(\mathbb{S}_k^q; \theta_k)} \\ \delta^{f_{k+1}^{q+1}} \end{bmatrix}, \quad (11)$$

where $\delta^{f_{k+1}^{q+1}} := f_k^s(\mathbf{s}_{k+1}^{q+1}; \theta_{k+1}^{q+1}) - f_k^s(\mathbf{s}_k^0; \theta_k^0)$. Solving (11) yields the closed form

$$\mathbf{a}_{k+1}^q = \frac{\mathbf{a}_k}{\hat{q}}, \quad \mathbf{a}_{k+1}^1 = \frac{\delta^{f_{k+1}^{q+1}}}{\zeta_{k+1}} \text{ and } \mathbf{a}_{k+1}^0 = \mathbf{a}_k^0.$$

3.2 Efficient Quadratic Subspace Models

We now consider two approaches to obtain subspace models that are nonlinear and able to address settings where less than a full quadratic ($\frac{1}{2}(q+1)(q+2)$) number of interpolation points are available. In both cases the strategy of reusing past interpolation points is similar to the linear case and is not further detailed here.

The first approach is a minimum Frobenius norm (MFN) model Hessian approach. At iteration k , we define \mathbb{S}_k^σ as above, where $\sigma \leq \nu(q) := \frac{1}{2}(q+1)(q+2)$. Consider the natural basis $\bar{\Phi}^{\nu(q)} := (\bar{\Phi}_L^q, \bar{\Phi}_Q^q)$ of \mathcal{P}_q^2 , where $\bar{\Phi}_L^q(\mathbf{s}) = (1, s_1, \dots, s_q)$ and $\bar{\Phi}_Q^q(\mathbf{s}) = (\frac{1}{2}s_1^2, s_1s_2, \dots, \frac{1}{2}s_q^2)$, and define, for any $\bar{\Phi}^q(\mathbf{s}) := (\phi^0(\mathbf{s}), \phi^1(\mathbf{s}), \dots, \phi^q(\mathbf{s}))$,

$$\mathbf{M}(\bar{\Phi}^q; \mathbb{S}_k^\sigma) = \begin{bmatrix} \phi^0(\mathbf{s}_k^0) & \phi^1(\mathbf{s}_k^0) & \dots & \phi^q(\mathbf{s}_k^0) \\ \phi^0(\mathbf{s}_k^1) & \phi^1(\mathbf{s}_k^1) & \dots & \phi^q(\mathbf{s}_k^1) \\ \vdots & \vdots & \ddots & \vdots \\ \phi^0(\mathbf{s}_k^\sigma) & \phi^1(\mathbf{s}_k^\sigma) & \dots & \phi^q(\mathbf{s}_k^\sigma) \end{bmatrix}.$$

The MFN q -dimensional subspace model \hat{m}_k is

$$\hat{m}_k(\mathbf{s}) = \alpha_L^\top \bar{\Phi}_L^q(\mathbf{s}) + \alpha_Q^\top \bar{\Phi}_Q^q(\mathbf{s}), \quad \mathbf{s} \in \mathbb{R}^q,$$

where (α_L, α_Q) is the solution of the optimization problem

$$\begin{aligned} & \min_{\alpha_L, \alpha_Q} \frac{1}{2} \|\alpha_Q\|_2^2 \\ & \text{such that } \sum_{i \in \{Q, L\}} \mathbf{M}(\bar{\Phi}_i^q; \mathbb{S}_k^\sigma) \alpha_i = f_k(\mathbb{S}_k^\sigma; \theta_k), \end{aligned}$$

with $f_k(\mathbb{S}_k^\sigma; \theta_k) := (f_k^s(\mathbf{s}_k^0; \theta_k^0), \dots, f_k^s(\mathbf{s}_k^\sigma; \theta_k^\sigma))^\top$.

Assuming the iteration k unsuccessful, the set $\mathbb{S}_{k+1}^{\sigma+1}$ is constructed analogously to \mathbb{S}_{k+1}^{q+1} so that (10) holds with q replaced by σ . Then the MFN $(q+1)$ -dimensional subspace model \hat{m}_{k+1} is given by

$$\hat{m}_{k+1}(\mathbf{s}) = \lambda_L^\top \bar{\Phi}_L^{q+1}(\mathbf{s}) + \lambda_Q^\top \bar{\Phi}_Q^{q+1}(\mathbf{s}), \quad \mathbf{s} \in \mathbb{R}^{q+1},$$

where (λ_L, λ_Q) is the solution of the optimization problem

$$\begin{aligned} & \min_{\lambda_L, \lambda_Q} \frac{1}{2} \|\lambda_Q\|_2^2 \\ \text{such that } & \sum_{i \in \{Q, L\}} \mathbf{M}(\bar{\Phi}_i^{q+1}; \mathbb{S}_{k+1}^{\sigma+1}) \lambda_i = \begin{bmatrix} f_k(\mathbb{S}_k^\sigma; \theta_k) \\ f_k^s(\mathbb{S}_{k+1}^{\sigma+1}; \theta_{k+1}^{\sigma+1}) \end{bmatrix}, \end{aligned}$$

so that only $f_k^s(\mathbb{S}_{k+1}^{\sigma+1}; \theta_{k+1}^{\sigma+1})$ at iteration $k+1$ is newly computed, while $f_k(\mathbb{S}_k^\sigma; \theta_k)$ from iteration k is reused.

Our second nonlinear model approach uses model Hessians that are diagonal, and hence there are $2q+1$ model parameters.

Let $\{e_q^i\}_{i=1}^q$ be the standard basis of \mathbb{R}^q . At iteration k , $\mathbb{S}_k^q := \{\mathbb{S}_k^0\} \cup \mathbb{S}_k^{q,1} \cup \mathbb{S}_k^{q,2}$, with $\mathbb{S}_k^0 = \mathbf{0}_q$, $\mathbb{S}_k^{q,1} := \{\mathbb{S}_k^i := \delta_k e_q^i\}_{i=1}^q$ and $\mathbb{S}_k^{q,2} := \{\mathbb{S}_k^{q+i} := -\delta_k e_q^i\}_{i=1}^q$. We consider $\Phi^q(\mathbf{s}) := (1, s_1, \dots, s_q, \frac{1}{2}s_1^2, \dots, \frac{1}{2}s_q^2)$ so that

$$\mathbf{M}(\Phi^q; \mathbb{S}_k^q) = \begin{bmatrix} 1 & \mathbf{0}_q^\top & \mathbf{0}_q^\top \\ \mathbf{1}_q & \delta_k \mathbf{I}_q & \frac{1}{2} \delta_k^2 \mathbf{I}_q \\ \mathbf{1}_q & -\delta_k \mathbf{I}_q & \frac{1}{2} \delta_k^2 \mathbf{I}_q \end{bmatrix} \in \mathbb{R}^{(2q+1) \times (2q+1)}. \quad (12)$$

Let $f_k(\mathbb{S}_k^q; \theta_k) := \begin{bmatrix} f_k(\mathbb{S}_k^{q,1}; \theta_k) \\ f_k(\mathbb{S}_k^{q,2}; \theta_k) \end{bmatrix}$, with $f_k(\mathbb{S}_k^{q,j}; \theta_k)$, $j = 1, 2$, defined as above. Then solving the linear system

$$\mathbf{M}(\Phi^q; \mathbb{S}_k^q) \mathbf{h}_{2q+1} = f_k(\mathbb{S}_k^q; \theta_k), \quad \mathbf{h}_{2q+1} = (h_0, \dots, h_{2q})^\top,$$

leads to a quadratic subspace model \hat{m}_k defined as in (5), where

$$\mathbf{f}_k = h_0, \quad \mathbf{g}_k = (h_1, \dots, h_q)^\top \text{ and } \hat{\mathbf{H}}_k = \begin{bmatrix} h_{q+1} & \cdots & \mathbf{0} \\ \vdots & \ddots & \vdots \\ \mathbf{0} & \cdots & h_{2q} \end{bmatrix}.$$

Assuming the iteration k unsuccessful, we define $\mathbf{M}(\Phi^{q+1}; \mathbb{S}_k^{q+1})$ using (12), and then \hat{m}_{k+1} by solving

$$\mathbf{M}(\Phi^{q+1}; \mathbb{S}_k^{q+1}) \ell_{2q+3} = \begin{bmatrix} f_k(\mathbb{S}_k^{q,1}; \theta_k) \\ f_k^s(\mathbb{S}_{k+1}^{q+1}; \theta_{k+1}^{q+1}) \\ f_k(\mathbb{S}_k^{q,2}; \theta_k) \\ f_k^s(\mathbb{S}_{k+1}^{2(q+1)}; \theta_{k+1}^{2(q+1)}) \end{bmatrix},$$

where $\mathbf{s}_{k+1}^{q+1} = -\mathbf{s}_{k+1}^{2(q+1)} = \hat{q} \delta_k \mathbf{e}_{q+1}^{q+1} \in \mathbb{R}^{q+1}$.

4 The ANASTAARS Algorithm

ANASTAARS is given by Algorithm 2 and inspired by STARS, as discussed in Section 2.2. The STARS instance in Algorithm 1 constructs a fixed-dimensional subspace model using newly generated interpolation sets and associated newly computed estimates of function values in every iteration. On the other hand, Algorithm 2 explicitly employs an adaptive subspace selection strategy, designed to occasionally (in particular, following every unsuccessful iteration) avoid such entirely new computations. Indeed, if iteration $k-1$ is successful or its q -dimensional subspace model is such that $q+1 > q_{\max}$ for some $q_{\max} \in \llbracket 2, d \rrbracket$, then a q_0 -dimensional subspace model, with $q_0 \in \llbracket 1, q_{\max} \rrbracket$, is constructed at iteration k using a new interpolation set \mathbb{S}_k and its associated function estimates. Otherwise, a $(q+1)$ -dimensional subspace model is constructed using a set $\mathbb{S}_k \subset \mathbb{R}^{q+1}$ obtained from $\mathbb{S}_{k-1} \subset \mathbb{R}^q$ combined with a new interpolation point $\mathbf{s}_k^{q+1} \in \mathbb{R}^{q+1}$, and their associated function estimates as detailed in Section 3. We note that the condition $q+1 > q_{\max}$ prevents the attempted construction of d' -dimensional subspace models, with $d' > d$, following an unsuccessful iteration.

As an additional feature, and inspired by noise-aware numerical optimization (e.g., [31, 38, 39]), ANASTAARS incorporates an estimate $\tilde{\varepsilon}_k$ of the noise level at \mathbf{x}_k into a modified ratio test $\tilde{\rho}_k$ of the reduction in the estimates and the reduction in the model. This alternative ratio, seen in Step 4 of Algorithm 1, is employed to determine whether an iteration is successful or not. We estimate $\tilde{\varepsilon}_k$ via the sample standard deviation; that is, for the computed number $\pi_k > 1$ of samples, $\tilde{\varepsilon}_k^2 := \frac{1}{\pi_k - 1} \sum_{\ell=1}^{\pi_k} (f_{\theta_\ell^0}(\mathbf{x}_k) - f_k^0)^2$, where $f_k^0 = \frac{1}{\pi_k} \sum_{\ell=1}^{\pi_k} f_{\theta_\ell^0}(\mathbf{x}_k)$.

[0] Initialization

Fix $\gamma > 1$, $\varepsilon_f, \eta_1 \in (0, 1)$, $\eta_2, \delta_{\max}, r > 0$, $\delta_0 \in (0, \delta_{\max})$, $q_{\max} \in \llbracket 2, d \rrbracket$, $q_0 \in \llbracket 1, q_{\max} \rrbracket$. Select $\mathbf{x}_0 \in \mathbb{R}^d$, set $F_{\text{flag}} = 0$, $k \leftarrow 0$ and $q \leftarrow q_0$.

[1] Construction of subspace model

If $F_{\text{flag}} = 0$ or $(q + 1) > q_{\max}$: reset $q \leftarrow q_0$, generate $\mathbf{Q}_k = \sqrt{\frac{d}{q}} \mathbf{U}_k \in \mathbb{R}^{d \times q}$ via Haar measure. Generate a poised set $\mathbb{S}_k \subset \mathbb{R}^q$. Build a q -dimensional subspace model $\hat{m}_k : \mathbb{R}^q \rightarrow \mathbb{R}$ using \mathbf{Q}_k and \mathbb{S}_k .

Otherwise: generate $\mu_k \in U_{k-1}^\perp$ from $\mathcal{U}(\mathbb{S}^{d-1})$, define $\mathbf{U}_k = [\mathbf{U}_{k-1}, \mu_k]$ and $\mathbf{Q}_k = \sqrt{\frac{d}{q+1}} \mathbf{U}_k \in \mathbb{R}^{d \times (q+1)}$ (see (9)).

Generate a new point $\mathbf{s}_k^{q+1} \in \mathbb{R}^{q+1}$ and obtain a poised set $\mathbb{S}_k \subset \mathbb{R}^{q+1}$ using \mathbb{S}_{k-1} and \mathbf{s}_k^{q+1} (see Section 3).

Build a $(q + 1)$ -dimensional subspace model $\hat{m}_k : \mathbb{R}^{q+1} \rightarrow \mathbb{R}$ using \mathbf{Q}_k , \mathbb{S}_k , function estimates associated to \mathbb{S}_{k-1} , and at \mathbf{s}_k^{q+1} (see Section 3). Set $q \leftarrow q + 1$ and $F_{\text{flag}} = 0$.

[2] Step calculation

Compute $\mathbf{s}_k \approx \arg \min \{\hat{m}_k(\mathbf{s}) : \mathbf{s} \in \mathbb{R}^q, \|\mathbf{s}\|_2 \leq \delta_k\}$ satisfying [18, (2.1)].

[3] Estimate computation

Compute ε_f -accurate estimates $f_k^0 \approx f(\mathbf{x}_k)$ and $f_k^s \approx f(\mathbf{x}_k + \mathbf{Q}_k \mathbf{s}_k)$ and obtain an estimate of noise level at \mathbf{x}_k through its standard deviation $\tilde{\varepsilon}_k$; if available, use samples from previous iterations.

[4] Updates

Compute $\tilde{\rho}_k = \frac{f_k^0 - f_k^s + r\tilde{\varepsilon}_k}{\hat{m}_k(\mathbf{0}) - \hat{m}_k(\mathbf{s}_k)}$

If $\tilde{\rho}_k \geq \eta_1$ and $\|\hat{\mathbf{g}}_k\|_2 \geq \eta_2 \delta_k$ (**success**): set $\mathbf{x}_{k+1} = \mathbf{x}_k + \mathbf{Q}_k \mathbf{s}_k$ and $\delta_{k+1} = \min \{\gamma \delta_k, \delta_{\max}\}$.

Otherwise (**failure**): $\mathbf{x}_{k+1} = \mathbf{x}_k$, $\delta_{k+1} = \gamma^{-1} \delta_k$ and $F_{\text{flag}} = 1$.

Update the iteration counter $k \leftarrow k + 1$ and go to [1].

Algorithm 2: New ANASTAARS algorithm.

5 Numerical experiments

The practical performance of a variant of Algorithm 2 using MFN subspace quadratic models (introduced in Section 3.2) is illustrated through experiments conducted on standard QAOA benchmarks. This variant, referred to as ANASTAARS-QD2, uses q -dimensional subspace models, with $q \in \llbracket q_0, q_{\max} \rrbracket$, where $q_0 = 2$ and $q_{\max} = d$. We set the other algorithmic parameters as $r = 1$, $\gamma = 2$, $\eta_1 = 0.01$, $\eta_2 = 0.9$, $\delta_{\max} = 5$, and $\delta_0 = 1$.

We compare ANASTAARS-QD2 with STARS-QD2, a variant of STARS using MFN 2-dimensional subspace quadratic models, and other methods previously tested in the literature for optimizing VQAs. More precisely, ANASTAARS-QD2 is also compared with PyBOBYQA [11], the implicit filtering method referred to as ImFil [28] (each as wrapped in scikit-quant [32]), NOMAD [33], ANATRA [31], and NEWUOA [44]. We note that while a variant of NOMAD is also wrapped in scikit-quant, we have chosen to use its version 4 because it is more recent and offers significant improvements. Moreover, for the same reasons provided in [31, Section 5.2], we intentionally omitted the optimizer SnobFit [24] wrapped in scikit-quant. We note that unlike [31], no comparison was made with the method of Simultaneous Perturbation Stochastic Approximation (SPSA) [53], not only due to its unavailability in Qiskit v0.46.1 (used in our experiments), but also because of its poor performance compared to the aforementioned optimizers for VQAs.

PyBOBYQA is an extension of the widely used DFO optimizer BOBYQA [45]. It is a model-based DFO optimizer that incorporates several heuristics aimed at enhancing the robustness of BOBYQA in the presence of noise. ImFil is a DFO method with a relatively intricate implementation that fundamentally operates as an inexact quasi-Newton approach using gradient estimates computed via central finite differences with initially large difference parameters. Intentionally designed to handle noisy cost functions, ImFil is a competitive method in general noise settings [31]. NOMAD is an implementation of the MADS [2] algorithm, which, unlike model-based methods, does not build explicit gradient or higher-order models. Instead, NOMAD explores a mesh of trial points and updates the incumbent if improvement is observed. Although not originally designed for noisy problems, NOMAD could potentially exhibit robustness to noise due to its model-free nature. ANATRA is a noise-aware, model-based trust-region algorithm designed for noisy DFO problems, such as those arising in VQAs. The key feature of ANATRA is its attempt to explicitly incorporate dynamic estimates of noise into its ρ test, as we mimic in ANASTAARS-QD2. NEWUOA is an iterative model-based DFO algorithm using interpolation models built with $2d + 1$ points. It employs a trust-region approach where only one interpolation point per iteration is altered.

In our first experiments we simulate QAOA MaxCut circuits with $p = 5$ layers in Qiskit [46], resulting in a set of

$2p = 10$ free parameters $(\gamma_1, \dots, \gamma_5, \beta_1, \dots, \beta_5)^\top =: \mathbf{x}$ in the $(d = 10)$ -dimensional Problem (3). We use the QASM simulator in Qiskit to simulate an ideal (state-vector) execution of the QAOA circuit in our experiments. By using the MaxCut cost function values suggested by QASM, we compute the shot-averaged estimates $f_k^j = \frac{1}{B} \sum_{\ell=1}^B f_{\theta_\ell^j}(\mathbf{x}_k)$, $j \in \{0, s\}$, used by Algorithm 2 and STARS-QD2. Here $B := \pi_k \in \{50, 100, 500, 1000\}$ denotes the per-evaluation shot count. We experiment with the MaxCut problem both on a toy graph and on standard benchmark Chvátal graphs, the former having a MaxCut value of 6 and the latter having a MaxCut value of 20.

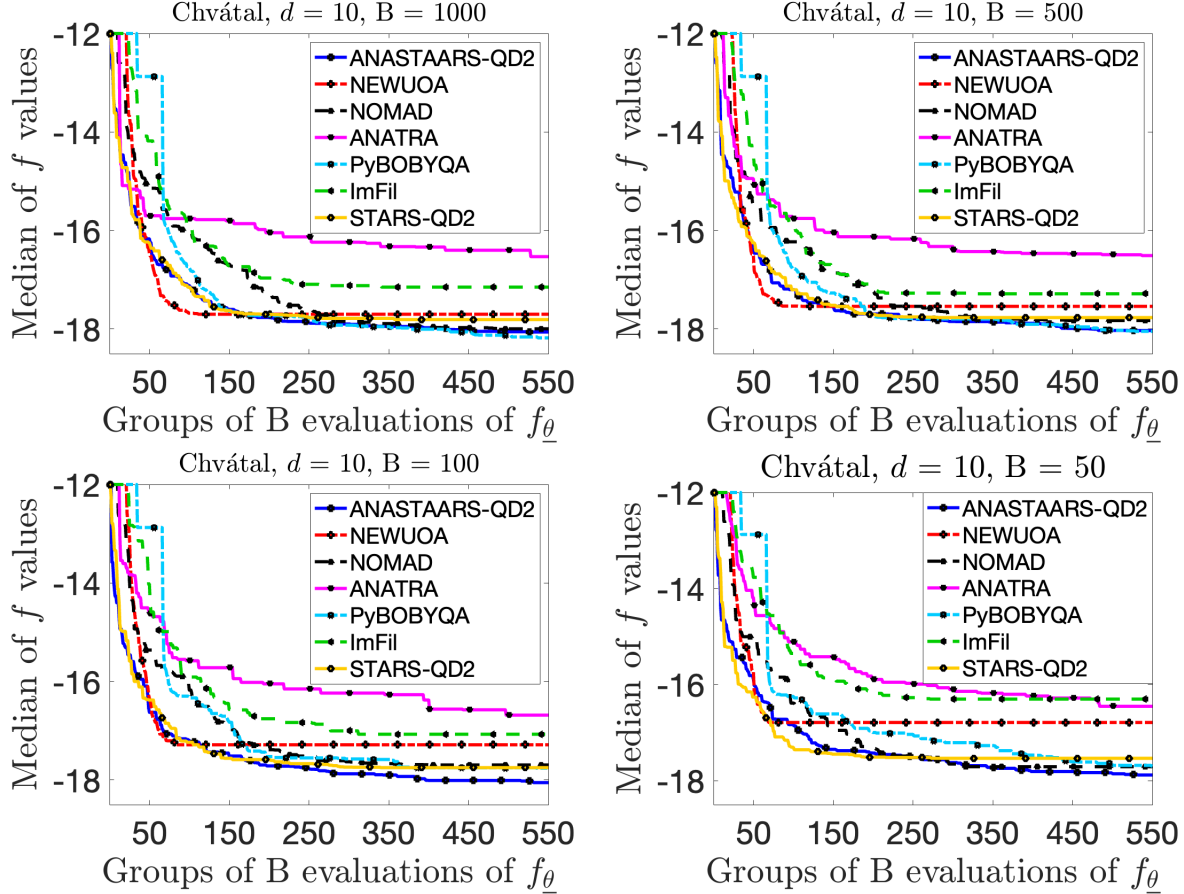


Figure 1: Median optimizer trajectories for the Chvátal graph with $d = 10$.

Figures 1 and 2 depict the median performance over 30 trials for each optimizer on the Chvátal and toy graphs, respectively. These figures show that ANASTAARS-QD2 is able to match the best long-term performance achieved by PyBOBYQA for these 10-dimensional problems. Unlike STARS-QD2, ANASTAARS-QD2 does not easily get stuck. This is likely due to the latter’s adaptive subspace strategy, which—following unsuccessful iterations—permits the use of higher-dimensional, potentially improved or more accurate models, thereby facilitating continued progress toward better solutions. For the largest shot count and total number of shots, Figure 3 depicts the variability across the 30 trials and illustrates that even at this large budget of shots, ANASTAARS-QD2 is among the best optimizers in terms of trial quantiles.

Our next set of experiments is aimed at testing optimizer scalability as the number p of QAOA layers increases. We show the behavior for $p = 5, \dots, 25$, corresponding to dimensions $d = 10, \dots, 50$. Following an initial downselection based on the scalability of the various methods, we report the performance of NEWUOA and NOMAD in addition to that of ANASTAARS-QD2. For different numbers of shots, Figures 4–7 show the median performance for the Chvátal graph, and Figures 8–11 show the median performance for the toy graph.

In the smallest budget cases (upper left in each figure), the lead of ANASTAARS-QD2 increases as the dimension increases. In the largest budget cases (lower left in each figure), ANASTAARS-QD2 maintains its lead over the other two optimizers as the dimension grows.

The results suggest that ANASTAARS-QD2 offers a way to consider larger-scale QAOA problems than are currently

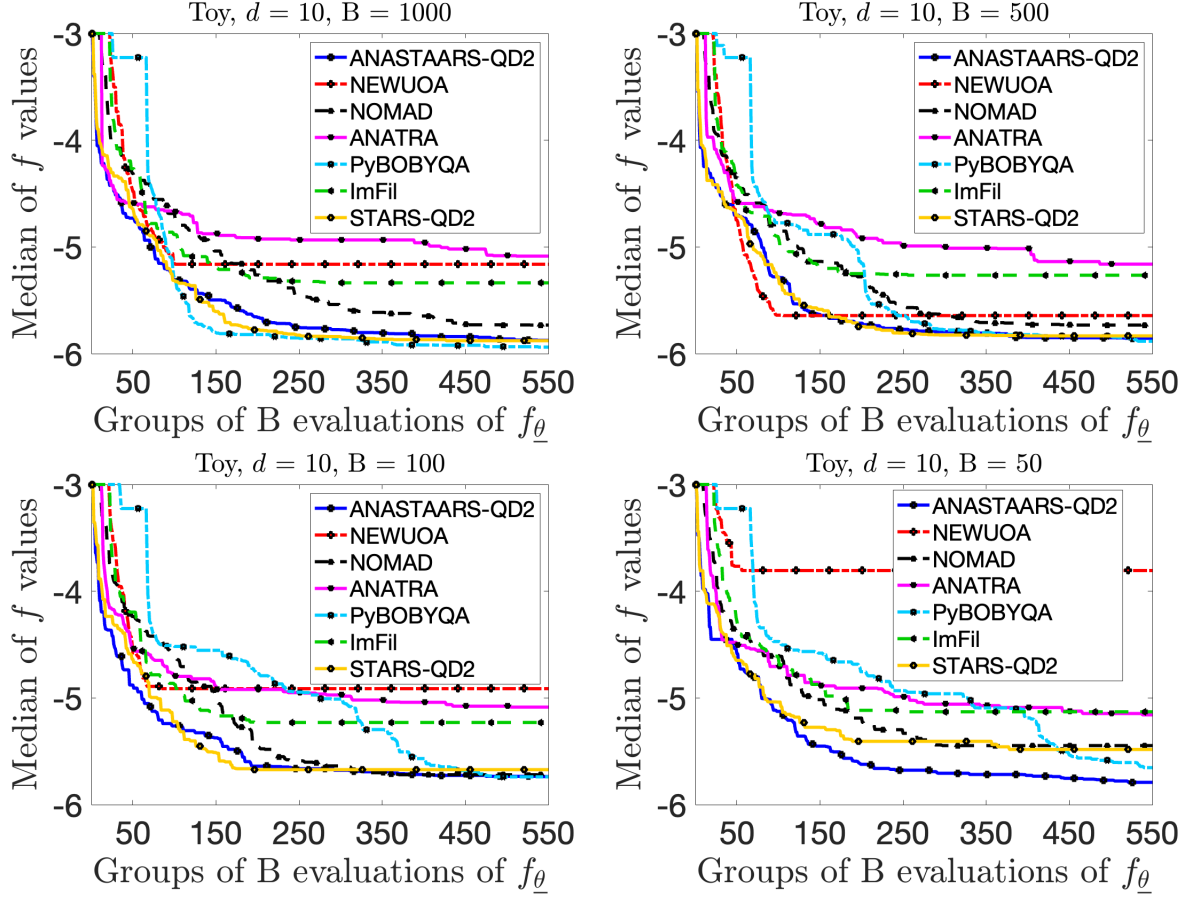


Figure 2: Median optimizer trajectories for the tov graph with $d = 10$.
 $d = 10, B = 1000$

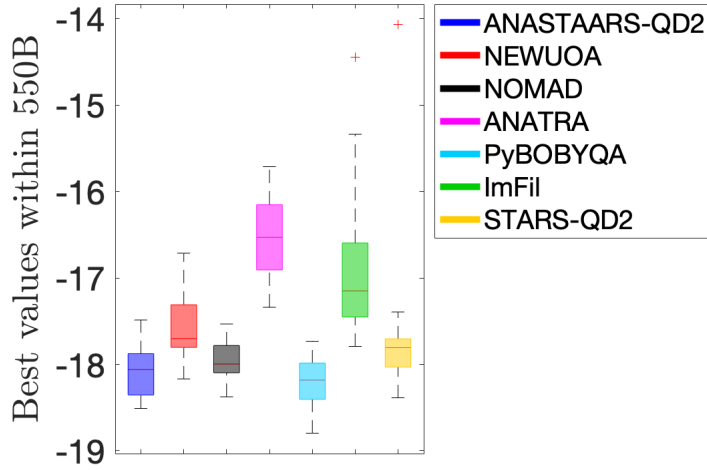


Figure 3: Distribution across the 30 trials for the Chvátal graph with $d = 10$ and $B = 1000$.

studied. By displaying consistent behavior across different numbers of shots used in the cost function estimates, the results also suggest that ANASTAARS-QD2 can be reliably deployed in different shot regimes.

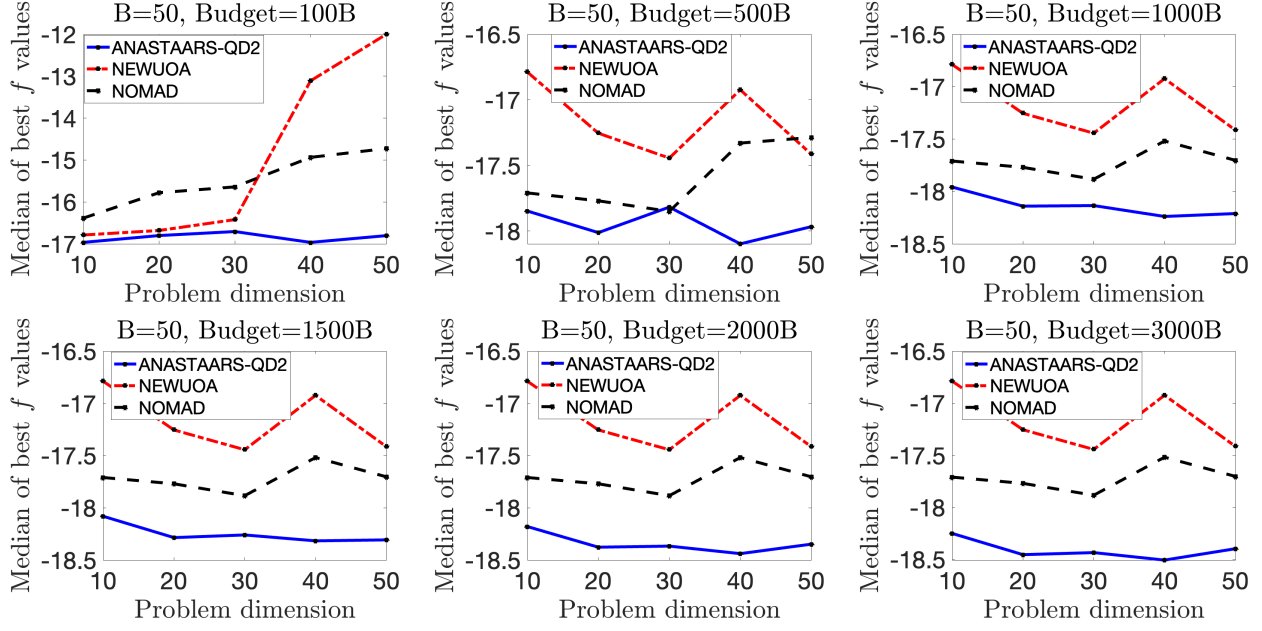


Figure 4: Chvátal scalability with 50 shots.

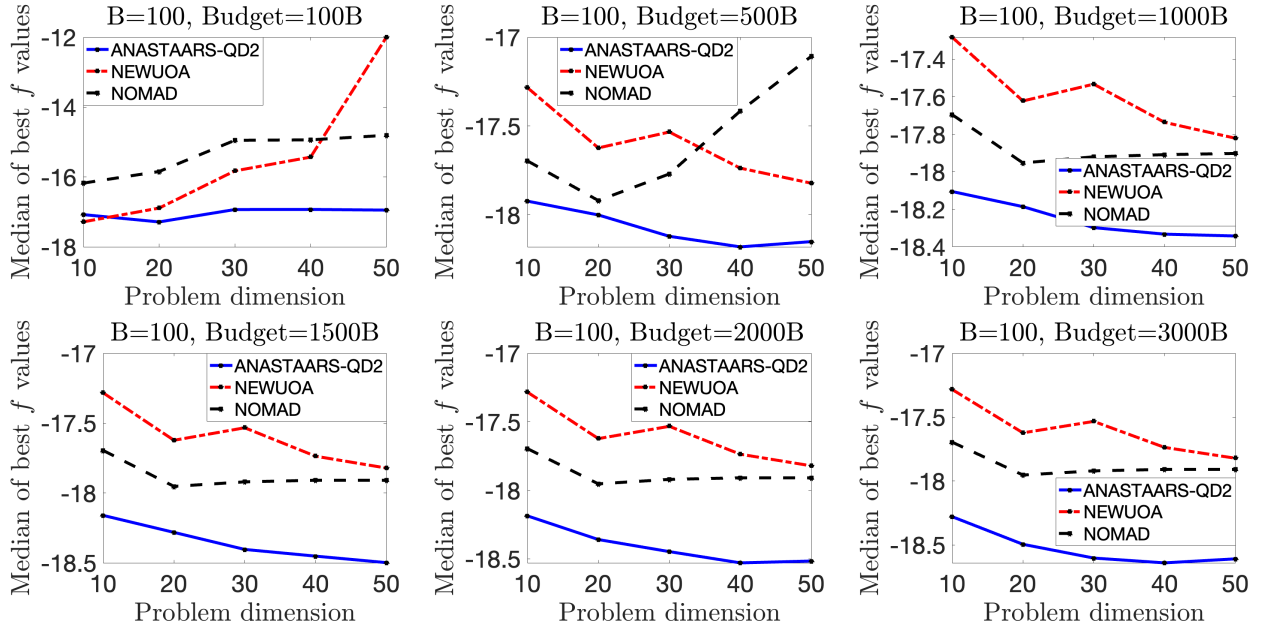


Figure 5: Chvátal scalability with 100 shots.

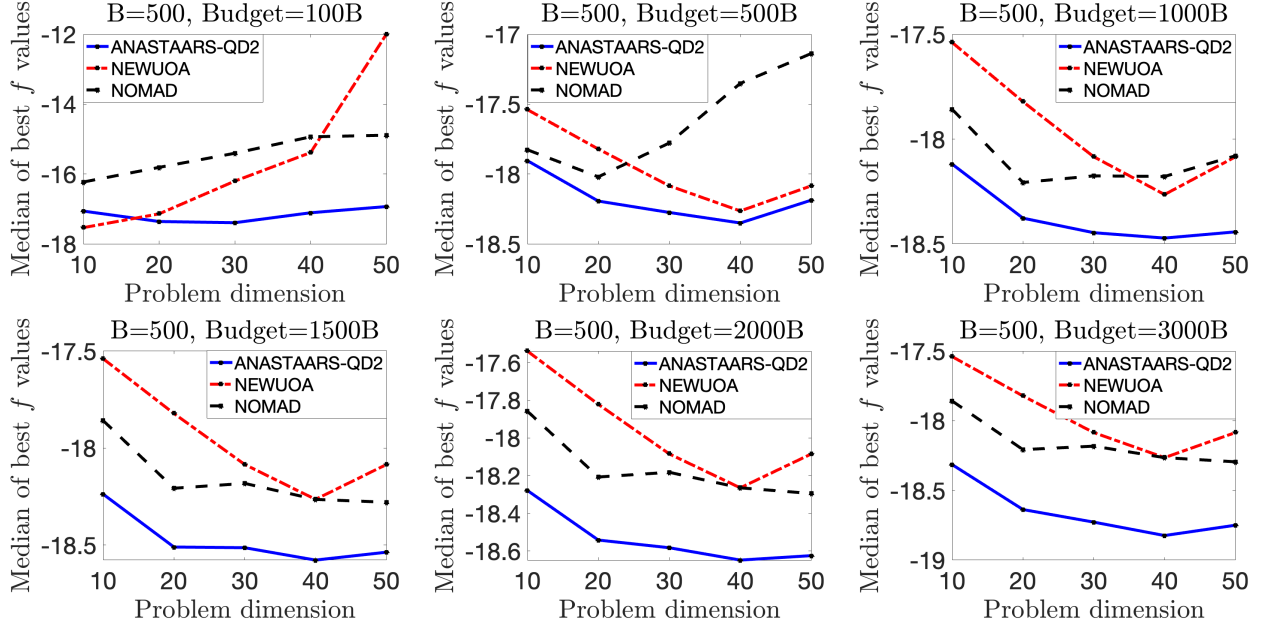


Figure 6: Chvátal scalability with 500 shots.

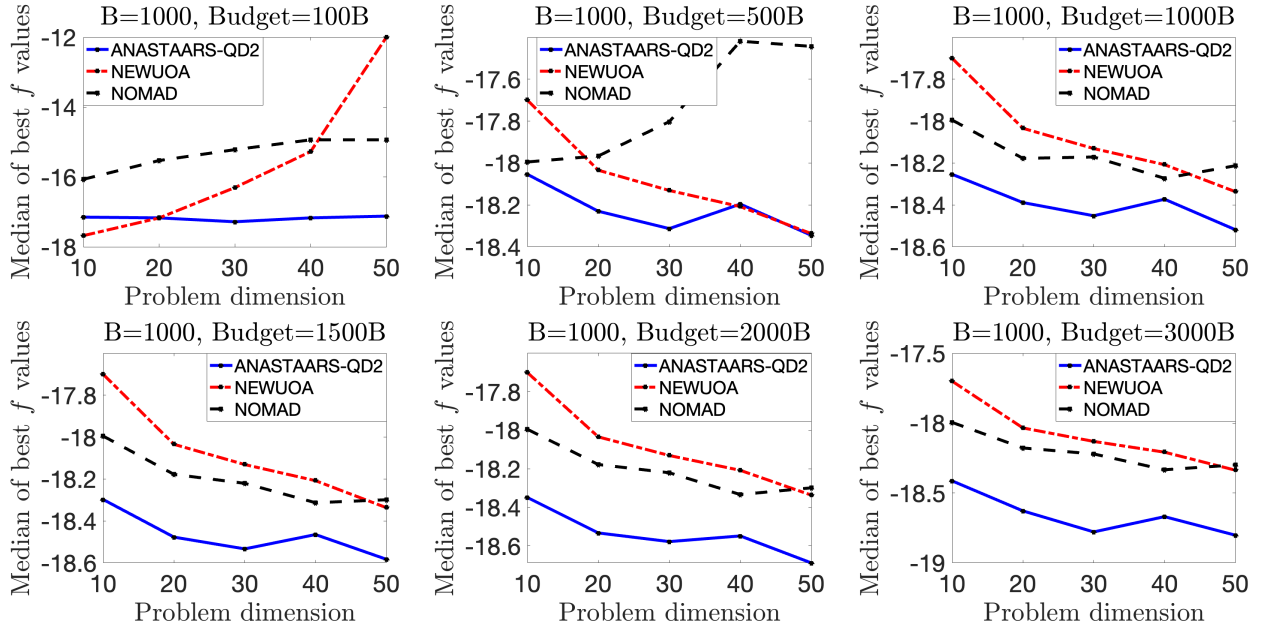


Figure 7: Chvátal scalability with 1000 shots.

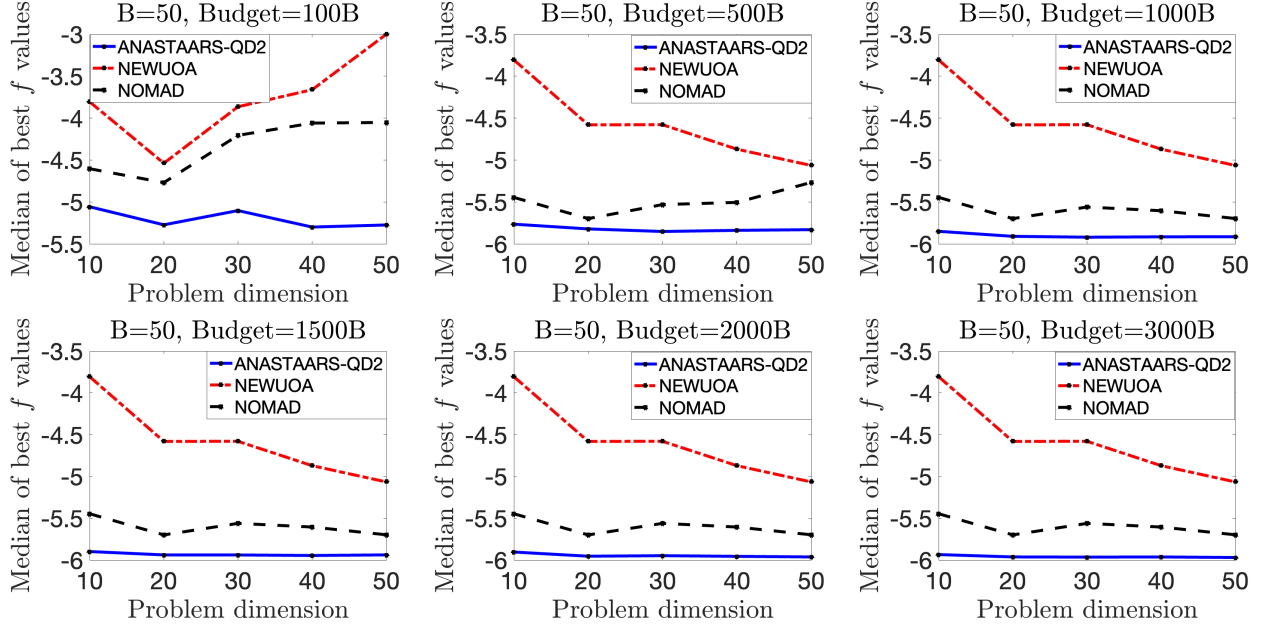


Figure 8: Toy scalability with 50 shots.

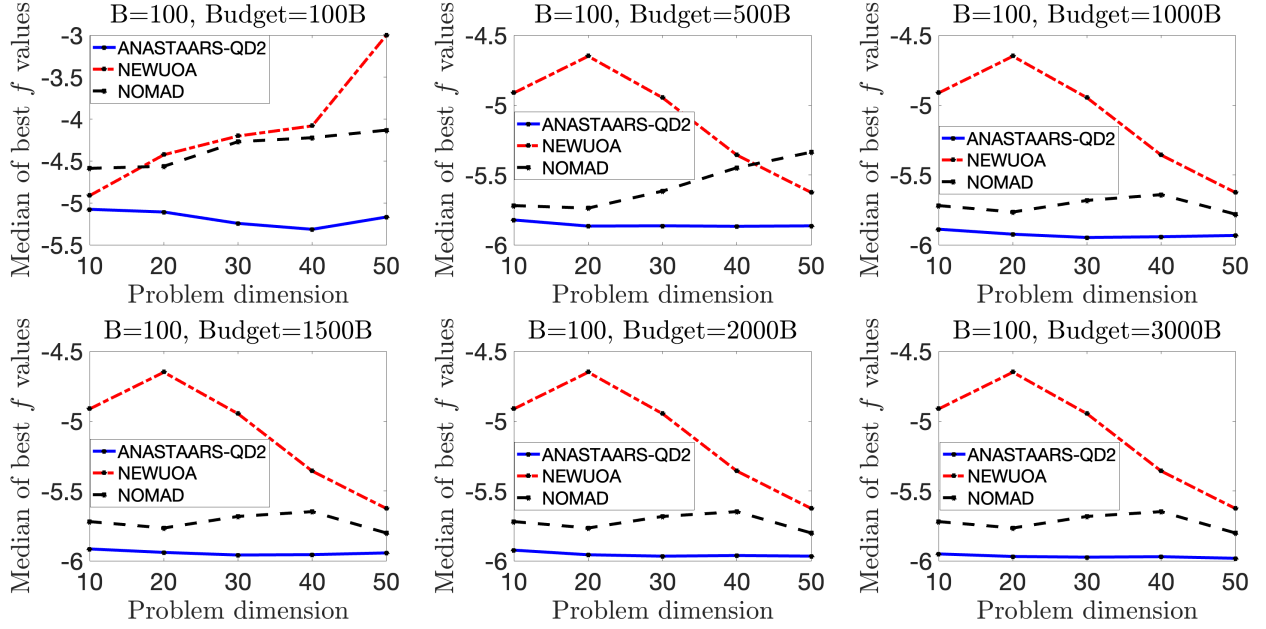


Figure 9: Toy scalability with 100 shots.

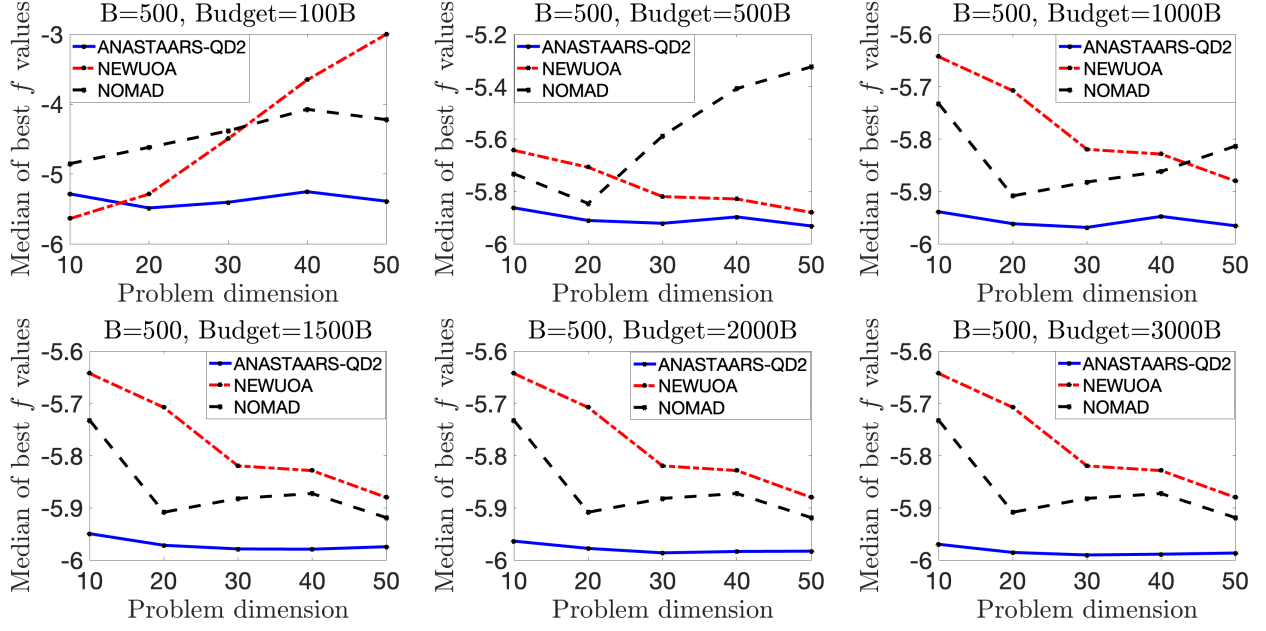


Figure 10: Toy scalability with 500 shots.

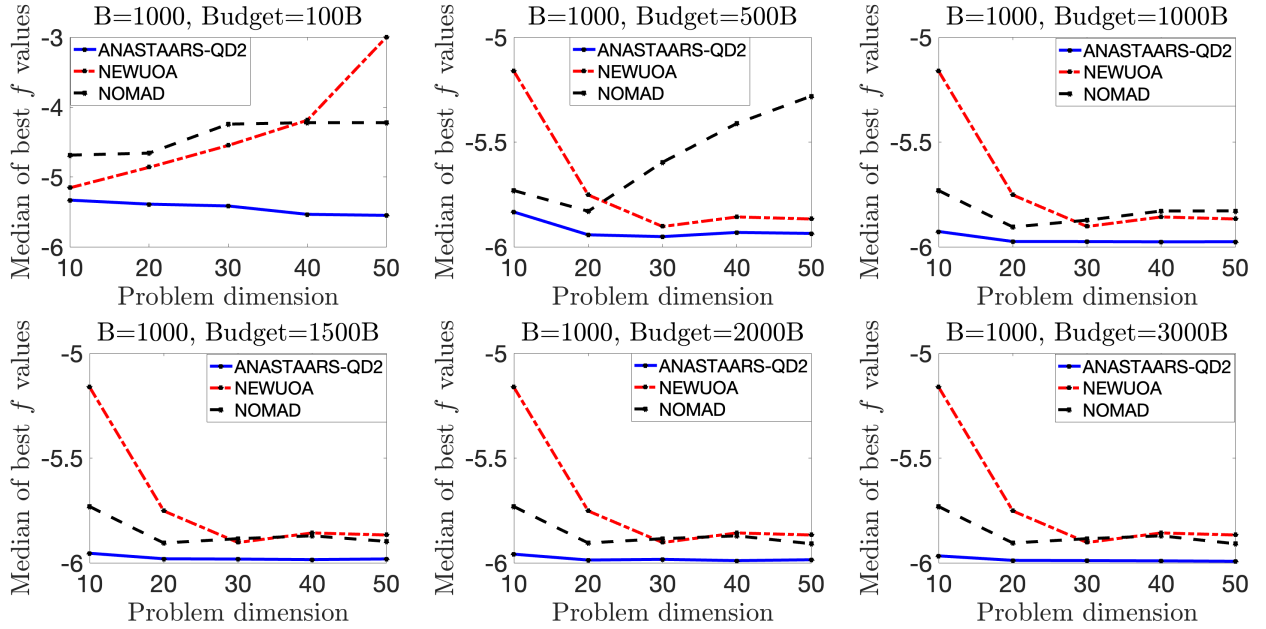


Figure 11: Toy scalability with 1,000 shots.

References

- [1] A. Arrasmith, L. Cincio, R. D. Somma, and P. J. Coles. Operator sampling for shot-frugal optimization in variational algorithms. *arXiv*, 2020. URL <https://arxiv.org/abs/2004.06252>.
- [2] C. Audet and J. Dennis, Jr. Mesh adaptive direct search algorithms for constrained optimization. *SIAM Journal on Optimization*, 17(1):188–217, 2006. doi:[10.1137/040603371](https://doi.org/10.1137/040603371).
- [3] C. Audet and W. Hare. *Derivative-Free and Blackbox Optimization*. Springer, Cham, Switzerland, 2017. doi:[10.1007/978-3-319-68913-5](https://doi.org/10.1007/978-3-319-68913-5).
- [4] C. Audet, K. J. Dzahini, M. Kokkolaras, and S. Le Digabel. Stochastic mesh adaptive direct search for black-box optimization using probabilistic estimates. *Computational Optimization and Applications*, 79(1):1–34, 2021. doi:[10.1007/s10589-020-00249-0](https://doi.org/10.1007/s10589-020-00249-0).
- [5] A. Bandeira, K. Scheinberg, and L. Vicente. Convergence of trust-region methods based on probabilistic models. *SIAM Journal on Optimization*, 24(3):1238–1264, 2014. doi:[10.1137/130915984](https://doi.org/10.1137/130915984).
- [6] K. Bharti, A. Cervera-Lierta, T. H. Kyaw, T. Haug, S. Alperin-Lea, A. Anand, M. Degroote, H. Heimonen, J. S. Kottmann, T. Menke, W.-K. Mok, S. Sim, L.-C. Kwek, and A. Aspuru-Guzik. Noisy intermediate-scale quantum algorithms. *Reviews of Modern Physics*, 94(1):015004, 2022. doi:[10.1103/RevModPhys.94.015004](https://doi.org/10.1103/RevModPhys.94.015004).
- [7] K. Blekos, D. Brand, A. Ceschini, C.-H. Chou, R.-H. Li, K. Pandya, and A. Summer. A review on quantum approximate optimization algorithm and its variants. *Physics Reports*, 1068:1–66, 2024. doi:[10.1016/j.physrep.2024.03.002](https://doi.org/10.1016/j.physrep.2024.03.002).
- [8] C. Bravo-Prieto, R. LaRose, M. Cerezo, Y. Subasi, L. Cincio, and P. J. Coles. Variational quantum linear solver. *Quantum*, 7:1188, 2023. doi:[10.22331/q-2023-11-22-1188](https://doi.org/10.22331/q-2023-11-22-1188).
- [9] R. Brent. *Algorithms for Minimization Without Derivatives*. Prentice-Hall, Englewood Cliffs, New Jersey, 1973. URL <http://store.doverpublications.com/0486419983.html>. Reissued in 2013 by Dover Publications, Mineola, New York.
- [10] C. Cartis and L. Roberts. Scalable subspace methods for derivative-free nonlinear least-squares optimization. *Mathematical Programming*, pages 1–64, 2022. doi:[10.1007/s10107-022-01836-1](https://doi.org/10.1007/s10107-022-01836-1).
- [11] C. Cartis, J. Fiala, B. Marteau, and L. Roberts. Improving the flexibility and robustness of model-based derivative-free optimization solvers. *ACM Transactions on Mathematical Software (TOMS)*, 45(3):1–41, 2019. doi:[10.1145/3338517](https://doi.org/10.1145/3338517).
- [12] C. Cartis, J. Fowkes, and Z. Shao. Randomised subspace methods for non-convex optimization, with applications to nonlinear least-squares. *arXiv*, (2211.09873), 2022. URL <https://arxiv.org/abs/2211.09873>.
- [13] C. Cartis, J. Fowkes, and Z. Shao. A randomised subspace Gauss–Newton method for nonlinear least-squares. *arXiv*, (2211.05727), 2022. URL <https://arxiv.org/abs/2211.05727>.
- [14] M. Cerezo, A. Arrasmith, R. Babbush, S. C. Benjamin, S. Endo, K. Fujii, J. R. McClean, K. Mitarai, X. Yuan, L. Cincio, and P. J. Coles. Variational quantum algorithms. *Nature Reviews Physics*, 3(9):625–644, 2021. doi:[10.1038/s42254-021-00348-9](https://doi.org/10.1038/s42254-021-00348-9).
- [15] R. Chen, M. Menickelly, and K. Scheinberg. Stochastic optimization using a trust-region method and random models. *Mathematical Programming*, 169(2):447–487, 2018. doi:[10.1007/s10107-017-1141-8](https://doi.org/10.1007/s10107-017-1141-8).
- [16] A. R. Conn, K. Scheinberg, and L. N. Vicente. *Introduction to Derivative-Free Optimization*. SIAM, Philadelphia, 2009. ISBN 978-0-898716-68-9. doi:[10.1137/1.9780898718768](https://doi.org/10.1137/1.9780898718768).
- [17] K. J. Dzahini. Expected complexity analysis of stochastic direct-search. *Computational Optimization and Applications*, 81(1):179–200, 2022. doi:[10.1007/s10589-021-00329-9](https://doi.org/10.1007/s10589-021-00329-9).
- [18] K. J. Dzahini and S. M. Wild. Stochastic trust-region algorithm in random subspaces with convergence and expected complexity analyses. *SIAM Journal on Optimization*, 34(3):2671–2699, 2024. doi:[10.1137/22M1524072](https://doi.org/10.1137/22M1524072).

- [19] K. J. Dzahini and S. M. Wild. Direct search for stochastic optimization in random subspaces with zeroth-, first-, and second-order convergence and expected complexity. *arXiv*, (2403.13320), 2024. URL <https://arxiv.org/abs/2403.13320>.
- [20] K. J. Dzahini and S. M. Wild. A class of sparse Johnson–Lindenstrauss transforms and analysis of their extreme singular values. *SIAM Journal on Matrix Analysis and Applications*, 46(1):416–438, 2025. doi:[10.1137/23M1605661](https://doi.org/10.1137/23M1605661).
- [21] K. J. Dzahini, M. Kokkolaras, and S. Le Digabel. Constrained stochastic blackbox optimization using a progressive barrier and probabilistic estimates. *Mathematical Programming*, 2022. doi:[10.1007/s10107-022-01787-7](https://doi.org/10.1007/s10107-022-01787-7).
- [22] E. Farhi, J. Goldstone, and S. Gutmann. A quantum approximate optimization algorithm. *arXiv*, (1411.4028), 2014. URL <https://arxiv.org/abs/1411.4028>.
- [23] Y. Ha, S. Shashaani, and M. Menickelly. Two-stage estimation and variance modeling for latency-constrained variational quantum algorithms. *INFORMS Journal on Computing*, 37(1):125–145, 2025. doi:[10.1287/ijoc.2024.0575](https://doi.org/10.1287/ijoc.2024.0575).
- [24] W. Huyer and A. Neumaier. SNOBFIT – Stable Noisy Optimization by Branch and Fit. *ACM Transactions on Mathematical Software*, 35(2):9:1–9:25, 2008. doi:[10.1145/1377612.1377613](https://doi.org/10.1145/1377612.1377613).
- [25] S. G. Johnson. The NLOpt nonlinear-optimization package. URL <https://nlopt.readthedocs.io/en/latest/>.
- [26] W. Johnson and J. Lindenstrauss. Extensions of Lipschitz mappings into a Hilbert space. *Contemporary Mathematics*, 26:189–206, 1984.
- [27] D. Kane and J. Nelson. Sparser Johnson–Lindenstrauss transforms. *Journal of the ACM*, 61(1):1–23, 2014. doi:[10.1145/2559902](https://doi.org/10.1145/2559902).
- [28] C. Kelley. *Implicit Filtering*. Society for Industrial and Applied Mathematics, Philadelphia, PA, 2011. doi:[10.1137/1.9781611971903](https://doi.org/10.1137/1.9781611971903).
- [29] J. M. Kübler, A. Arrasmith, L. Cincio, and P. J. Coles. An adaptive optimizer for measurement-frugal variational algorithms. *Quantum*, 4:263, 2020. doi:[10.22331/q-2020-05-11-263](https://doi.org/10.22331/q-2020-05-11-263).
- [30] J. Larson, M. Menickelly, and S. Wild. Derivative-free optimization methods. *Acta Numerica*, 28:287–404, 2019. doi:[10.1017/S0962492919000060](https://doi.org/10.1017/S0962492919000060).
- [31] J. Larson, M. Menickelly, and J. Shi. A novel noise-aware classical optimizer for variational quantum algorithms. *arXiv*, (2401.10121), 2024. URL <https://arxiv.org/abs/2401.10121>.
- [32] W. Lavrijsen, A. Tudor, J. Müller, C. Iancu, and W. De Jong. Classical optimizers for noisy intermediate-scale quantum devices. In *2020 IEEE International Conference on Quantum Computing and Engineering (QCE)*, pages 267–277, 2020. doi:[10.1109/QCE49297.2020.00041](https://doi.org/10.1109/QCE49297.2020.00041).
- [33] S. Le Digabel. Algorithm 909: NOMAD: Nonlinear optimization with the MADS algorithm. *ACM Transactions on Mathematical Software*, 37(4):44:1–44:15, 2011. doi:[10.1145/1916461.1916468](https://doi.org/10.1145/1916461.1916468).
- [34] J. R. McClean, J. Romero, R. Babbush, and A. Aspuru-Guzik. The theory of variational hybrid quantum-classical algorithms. *New Journal of Physics*, 18(2):023023, 2016. doi:[10.1088/1367-2630/18/2/023023](https://doi.org/10.1088/1367-2630/18/2/023023).
- [35] E. S. Meckes. *The Random Matrix Theory of the Classical Compact Groups*. Cambridge Tracts in Mathematics. Cambridge University Press, Cambridge, 2019. doi:[10.1017/9781108303453](https://doi.org/10.1017/9781108303453).
- [36] M. Menickelly. Avoiding geometry improvement in derivative-free model-based methods via randomization. *arXiv*, 2023. URL <https://arxiv.org/abs/2305.17336>.
- [37] M. Menickelly. Augmenting subspace optimization methods with linear bandits. *arXiv*, 2024. URL <https://arxiv.org/abs/2412.14278>.
- [38] M. Menickelly, Y. Ha, and M. Otten. Latency considerations for stochastic optimizers in variational quantum algorithms. *Quantum*, 7:949, 2023. doi:[10.22331/q-2023-03-16-949](https://doi.org/10.22331/q-2023-03-16-949).

- [39] M. Menickelly, S. M. Wild, and M. Xie. A stochastic quasi-Newton method in the absence of common random numbers. Technical Report 2302.09128, arXiv, 2023. URL <https://arxiv.org/abs/2302.09128>.
- [40] J. Nelder and R. Mead. A simplex method for function minimization. *The Computer Journal*, 7(4):308–313, 1965. doi:[10.1093/comjnl/7.4.308](https://doi.org/10.1093/comjnl/7.4.308). URL <http://comjnl.oxfordjournals.org/content/7/4/308.abstract>.
- [41] A. Pellow-Jarman, I. Sinayskiy, A. Pillay, and F. Petruccione. A comparison of various classical optimizers for a variational quantum linear solver. *Quantum Information Processing*, 20(6):202, 2021. doi:[10.1007/s11128-021-03140-x](https://doi.org/10.1007/s11128-021-03140-x).
- [42] M. Powell. A Direct Search Optimization Method That Models the Objective and Constraint Functions by Linear Interpolation. In S. Gomez and J.-P. Hennart, editors, *Advances in Optimization and Numerical Analysis*, volume 275 of *Mathematics and Its Applications*, pages 51–67. Springer, 1994. doi:[10.1007/978-94-015-8330-5_4](https://doi.org/10.1007/978-94-015-8330-5_4).
- [43] M. Powell. Direct search algorithms for optimization calculations. *Acta Numerica*, 7:287–336, 1998.
- [44] M. Powell. The NEWUOA software for unconstrained optimization without derivatives. In P. Pardalos, G. Pillo, and M. Roma, editors, *Large-Scale Nonlinear Optimization*, volume 83 of *Nonconvex Optimization and Its Applications*, pages 255–297. Springer, 2006. ISBN 978-0-387-30065-8. doi:[10.1007/0-387-30065-1_16](https://doi.org/10.1007/0-387-30065-1_16).
- [45] M. Powell. The BOBYQA algorithm for bound constrained optimization without derivatives. Technical Report DAMTP 2009/NA06, Department of Applied Mathematics and Theoretical Physics, University of Cambridge, Silver Street, Cambridge CB3 9EW, England, 2009.
- [46] Qiskit Contributors. Qiskit: An open-source framework for quantum computing. *Zenodo: Geneva, Switzerland*, 2023. doi:[10.5281/zenodo.2573505](https://doi.org/10.5281/zenodo.2573505).
- [47] L. Roberts and C. W. Royer. Direct search based on probabilistic descent in reduced spaces. *SIAM Journal on Optimization*, 33(4):3057–3082, 2023. doi:[10.1137/22M1488569](https://doi.org/10.1137/22M1488569).
- [48] T. Rowan. *Functional Stability Analysis of Numerical Algorithms*. PhD thesis, The University of Texas at Austin, 1990. URL <http://citeseerx.ist.psu.edu/viewdoc/summary?Doi=10.1.1.31.5708>.
- [49] Z. Shao. *On Random Embeddings and their Applications to Optimization*. PhD thesis, University of Oxford, 2022. URL <https://arxiv.org/abs/2206.03371>.
- [50] S. Shashaani, F. Hashemi, and R. Pasupathy. ASTRO-DF: A class of adaptive sampling trust-region algorithms for derivative-free stochastic optimization. *SIAM Journal on Optimization*, 28(4):3145–3176, 2018. doi:[10.1137/15M1042425](https://doi.org/10.1137/15M1042425).
- [51] R. Shaydulin, I. Safro, and J. Larson. Multistart methods for quantum approximate optimization. In *2019 IEEE High Performance Extreme Computing Conference (HPEC)*, pages 1–8, 2019. doi:[10.1109/HPEC.2019.8916288](https://doi.org/10.1109/HPEC.2019.8916288).
- [52] R. Shaydulin, P. C. Lotshaw, J. Larson, J. Ostrowski, and T. S. Humble. Parameter transfer for quantum approximate optimization of weighted maxcut. *ACM Transactions on Quantum Computing*, 4(3):1–15, 2023. doi:[10.1145/3584706](https://doi.org/10.1145/3584706).
- [53] J. C. Spall. Multivariate stochastic approximation using a simultaneous perturbation gradient approximation. *IEEE Transactions on Automatic Control*, 37(3):332–341, 1992. doi:[10.1109/9.119632](https://doi.org/10.1109/9.119632).
- [54] Z. Wang, S. Hadfield, Z. Jiang, and E. G. Rieffel. Quantum approximate optimization algorithm for maxcut: A fermionic view. *Physical Review A*, 97(2):022304, 2018. doi:[10.1103/PhysRevA.97.022304](https://doi.org/10.1103/PhysRevA.97.022304).
- [55] D. Wierichs, J. Izaac, C. Wang, and C. Y.-Y. Lin. General parameter-shift rules for quantum gradients. *Quantum*, 6:677, 2022. doi:[10.22331/q-2022-03-30-677](https://doi.org/10.22331/q-2022-03-30-677).

The submitted manuscript has been created by UChicago Argonne, LLC, Operator of Argonne National Laboratory (“Argonne”). Argonne, a U.S. Department of Energy Office of Science laboratory, is operated under Contract No. DE-AC02-06CH11357. The U.S. Government retains for itself, and others acting on its behalf, a paid-up nonexclusive, irrevocable worldwide license in said article to reproduce, prepare derivative works, distribute copies to the public, and perform publicly and display publicly, by or on behalf of the Government. The Department of Energy will provide public access to these results of federally sponsored research in accordance with the DOE Public Access Plan <http://energy.gov/downloads/doe-public-access-plan>.